

## Structure of the self-trapped exciton and nascent Frenkel pair in alkali halides: An *ab initio* study

K. S. Song

*Department of Physics, University of Ottawa, Ottawa, Ontario, Canada K1N 6N5*

R. C. Baetzold

*Corporate Research Laboratories, Eastman Kodak Company, Rochester, New York 14650*

(Received 30 January 1992)

Adiabatic-potential-energy surfaces of the self-trapped exciton (STE) of both the spin-singlet and -triplet states in NaF, NaCl, and NaBr are calculated with use of *ab initio* Hartree-Fock cluster methods. In all cases, there is clear evidence of adiabatic instability in the on-center geometry. The STE undergoes a spontaneous symmetry-breaking relaxation, resulting in a structure which is equivalent to an *F-H* center pair (a Frenkel defect pair in the anion sublattice). The potential energy is remarkably flat, to within about 0.2 eV, for further separation of the *H* center from the *F* center up to a distance of about 3 Å, the largest distance attained in this study. In view of the flat nature of the excited-state energy surface, and given the difficulties inherent in an *ab initio* computation, the calculated recombination energies are found to be within an acceptable range of values when compared with experiment for both the  $\sigma$  and  $\pi$  bands. From this work, the initial state of the  $\sigma$  emission band is attributed to the singlet STE of the lowest orbital state. On the basis of the adiabatic potential energies obtained in this work, a mechanism of  $\pi$ -band quenching is proposed.

### I. INTRODUCTION

Several recent *ab initio* Hartree-Fock cluster calculations<sup>1,2</sup> have confirmed the off-center structure of the self-trapped exciton (STE) in alkali halides which was predicted earlier by Song and co-workers.<sup>3,4</sup> An increasing array of experimental data is in support of this structure. The experiments include ultrafast time-resolved spectroscopic studies of transient *F*-center formation,<sup>5,6</sup> resonant Raman scattering of the STE,<sup>7</sup> detailed studies of  $\pi$ -band line shape,<sup>8</sup> and luminescence studies<sup>9</sup> to name a few. According to this model, the triplet STE which is responsible for the  $\pi$  emission bands in all alkali halides is not in the  $V_K$  center configuration with an excited electron in an *s*-like orbital (the on-center model). Rather this configuration undergoes a spontaneous symmetry-breaking distortion and forms at equilibrium a STE which is a more or less well formed *F-H* pair (a Frenkel defect pair in the anion sublattice).

It has been deduced that the lowest STE state and the ground state of the *F-H* pair are on the same adiabatic potential surface since an anticorrelation between  $\pi$ -band intensity and *F*-center formation is observed in a number of systems such as NaCl, NaBr, KI, and RbI (Ref. 10) as a function of temperature. On the other hand, it was the general belief until the work of Song, Leung, and Williams in 1989 (Ref. 3) that there would be a very substantial potential barrier on the trajectory of the STE (on center) leading to the nearest-neighbor *F-H* pair geometry because of the repulsive potential of the pair of alkali ions straddling the  $V_K$  center.<sup>11</sup> This barrier was evaluated to be larger than 2 eV in a calculation performed by Itoh, Stoneham, and Harker on KCl using the complete neglect of differential overlap (CNDO) method

in conjunction with the HADES code.<sup>12</sup>

The prediction that the STE is strongly unstable in the assumed geometry having  $D_{2h}$  symmetry and that the potential energy remains flat during further separation of the electron and hole constituted a fundamental departure from the accepted view of the structure of the STE in alkali halides which was established since the work of Kabler in 1964.<sup>13</sup> The self-trapping of an exciton in these wide band-gap materials has major effects on luminescence (Stokes shift, lifetime etc.), transport (hopping diffusion), and radiation defect formation among other properties.

In this paper we report a detailed study of the adiabatic-potential-energy surface (APES) of the STE obtained for NaF, NaCl, and NaBr using for the most part an *ab initio* Hartree-Fock cluster code CADPAC.<sup>14</sup> The systems studied, NaF, NaCl, and NaBr, belong to distinct groups in several important aspects. The energy required to create an *F* center under x-ray or electron-beam irradiation at liquid-He temperature decreases in the order NaBr, NaCl, and NaF by as much as four orders of magnitude. On the other hand, the Stokes shift of the  $\pi$  bands increases in the order NaBr, NaCl, and NaF by more than a factor of 2. Indeed, Rabin and Klick<sup>15</sup> have established a correlation between the energy required to create an *F* center at liquid-He temperature and a geometric parameter  $S/D$ . They found that *F* centers are very easily formed when  $S/D > 0.45$  and require much larger energy when  $S/D < 0.45$ .  $S$  represents the space between two adjacent halide ions in the (110) axis and  $D$  is the diameter of a neutral halide atom. Recently, Kan'no, Tanaka, and Hayashi<sup>9</sup> have plotted the ratio of the  $\pi$ -band Stokes shift to the free exciton absorption energy against  $S/D$  and observed that there are three types

of STE in alkali halides. Type I (which includes NaBr and NaI) with small Stokes shift of about 25% of the free exciton absorption energy fits for  $S/D < 0.3$ . Type II (which includes NaCl, KI, and RbI) with intermediate Stokes shift fits in the range of  $S/D$  between 0.3 and 0.4. Finally, type III (which comprises NaF, KF, RbF, KCl, RbCl, KBr, and RbBr) with Stokes shift as large as 76% of the free exciton absorption energy fits for  $S/D > 0.47$ .

In the present study a relatively small cluster of atoms is embedded inside a large array of fixed point charges. The cluster used is  $\text{Na}_{10}\text{X}_2$ , but for an extended range of electron and hole separations, we have also studied the  $\text{Na}_{14}\text{F}_3$  cluster. Keeping the position of one of the halide ions fixed on the (110) axis at a number of points, the position of the remainder of the ions in the quantum cluster has been optimized. The total energy of the cluster is then plotted as a function of the coordinate  $\Delta Q_2$ , which represents the off-center shift of the molecular ion  $\text{X}_2^-$  from the on-center position. We have studied both the spin-triplet state of the STE, which is responsible for the  $\pi$  emission bands, and the spin-singlet state of the lowest-energy open shell, which is believed to be responsible for the  $\sigma$  emission bands.

The APES we calculated shows that (i) for both spin states there is clear instability of the system in the  $D_{2h}$  symmetry. (ii) The APES remains very flat to within about 0.2 eV for displacements as large as we could study with the small cluster  $\text{Na}_{10}\text{X}_2$  (up to  $\Delta Q_2 \cong 1.5 \text{ \AA}$ ). For NaF, results with the larger  $\text{Na}_{14}\text{F}_3$  cluster show that the energy surface remains flat to within about 0.2 eV for displacement up to the second-nearest-neighbor  $F$ - $H$  pair geometry. (iii) The excited electron localizes on the nascent anion vacancy in all cases studied. The hole is strongly polarized such that it is more localized on the halide ion, which is proximal to the localized electron.

On comparing these results with those reported by Shluger *et al.* on KCl,<sup>2</sup> we note that there is basic agreement on the points (i) and (iii) enumerated above. These workers have found that the APES of the triplet STE in KCl reaches a minimum for  $\Delta Q_2 \cong 0.9 \text{ \AA}$  and remains relatively flat until  $\Delta Q_2 \cong 1.2 \text{ \AA}$ . However, when  $\Delta Q_2 \cong 1.5 \text{ \AA}$  is reached, a barrier of more than 0.7 eV is encountered. On the basis of this work, they argued subsequently that the STE's experimentally studied in the past are unspecified  $F$ - $H$  pairs, which are further separated from the STE they obtained by a potential barrier of substantial magnitude.<sup>16</sup> This disagreement between the two *ab initio* studies is of significant importance, not only concerning the precise identity of the STE, which has been the subject of extensive investigations, but also for its implication in primary defect formation under ionizing radiation.

We have therefore made a careful analysis of this problem. In particular, we have repeated more calculations on NaF with the CADPAC code, but using several sets of floating Gaussian orbitals (FGO) basis distributed at the interstices surrounding the molecular ion, as has been used in Ref. 2. NaF is a crystal similar to KCl in terms of classification of the STE luminescence and the efficient yield of  $F$  centers at very low temperature.<sup>9,17</sup> We find

that with ten FGO's distributed at the interstices, a potential barrier of about 0.4 eV appears near  $\Delta Q_2 \cong 1 \text{ \AA}$ . With the two FGO's placed near the anion vacancies used in our earlier work,<sup>1</sup> this barrier is reduced to about 0.2 eV. When the interstitial FGO's and the two vacancy-centered FGO's are used in combination, the barrier disappears altogether. The use of the FGO positioned near the anion sites is, therefore, a crucial factor in obtaining flat APES. In an attempt to estimate the contribution of the polarization of the lattice outside the quantum cluster, we have also performed calculations using the ICECAP code taking the position of quantum-mechanical ions obtained from the CADPAC computation. We will describe these codes in later sections.

In LiCl, Shluger, Grimes, and Catlow have reported an unusual structure.<sup>18</sup> Although an off-center STE is obtained, the excited electron is found in a diffuse orbital around the chlorine atom at the opposite end across the molecular ion from the nascent anion vacancy. This structure is surprising, because it has been argued that the localization of the excited electron on the vacated anion site is the driving force of the adiabatic instability.<sup>17,19</sup> Our present study of LiCl shows a structure similar to those already found in other alkali halides, with the electron localized on the anion vacancy. The APES remains extremely flat after the initial energy drop from the on-center geometry. We noted that a structure similar to that of Ref. 18 can result when the self-consistent-field (SCF) procedure in the unrestricted Hartree-Fock (UHF) calculation was started for the triplet state without first performing the closed-shell ground-state calculation and using the obtained eigenvectors as the starting point. Even when such a structure resulted, its energy was found to be higher than that of the *normal* off-center STE by about 0.9 eV.

This paper is organized in the following way. In Sec. II we describe the method of calculation, especially the embedding procedure and the basis used. The APES of the triplet and singlet state STE in NaF, NaCl, and NaBr obtained using the CADPAC code are presented in Sec. III A. Luminescence energies calculated for the singlet and triplet STE's are compared with experimental data of  $\sigma$  and  $\pi$  bands, respectively. Section III B is devoted to an analysis of the various choices of FGO basis sets and their effect on the APES which connects the STE with  $F$ - $H$  pairs. We show that electron localization and the energy barrier on the APES are sensitively dependent on the choice of the FGO, which is employed to augment the wave function of the excited electron. In Sec. III C we discuss the STE state with delocalized electron reported for LiCl in Ref. 18. Finally in Sec. III D, based on the present work, we make a brief proposition concerning the mechanisms of  $\pi$  luminescence quenching observed in various alkali halides. A short conclusion is given in Sec. IV.

## II. METHOD OF CALCULATION

The quantum-mechanical cluster embedded within an array of fixed point ions of charge  $\pm 1$  is treated with the

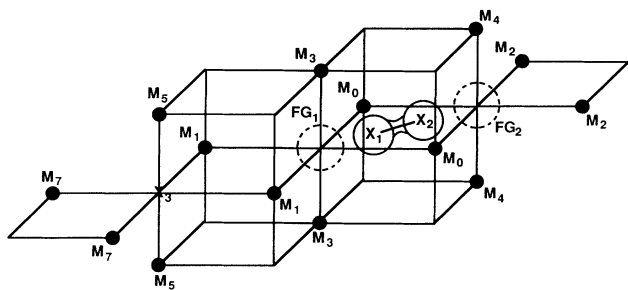


FIG. 1. Geometry of the cluster  $M_{14}X_3$  used in the study of NaF. In the smaller cluster  $M_{10}X_2$  used for NaF, NaCl, and NaBr, ions  $X_3$ ,  $M_5$ , and  $M_7$  are absent.

CADPAC code.<sup>14</sup> Clusters varying in size from  $M_{10}X_2$ ,  $M_{14}X_3$ , and  $M_{10}X_4$  ( $M$  represents a metal ion,  $X$  represents a halide ion) with the NaCl structure were considered and shown in Fig. 1. The fixed point ions are arranged at the regular ionic sites in a perfect lattice and centered spherically about the midpoint of the molecular ion  $X_2^-$  in the  $V_K$  center geometry. The number of point ions is 888 or 1308 in the case of  $M_{10}X_2$  resulting in a net neutral charge when both quantum-mechanical and point ion arrays are considered together. In order to prevent the surface atoms of the quantum cluster from undergoing unphysical displacements in the course of geometry optimization, Born-Mayer repulsive potentials are included between all of the fixed ions adjacent to and interacting with the quantum-mechanical ions. If the quantum cluster is large enough, it is possible to fix the quantum-mechanical ions at the surface and still get a meaningful geometry optimization. In our case, this was not practical as it would leave only the two halide ions to relax.

We tested the quality of the basis functions employed and the embedding procedure by examining the stability of the  $M_{10}X_2$  quantum cluster. A full geometry optimization of the ground-state cluster is performed by the analytic gradient method in CADPAC. Only minor displacements of ions from the perfect lattice sites are observed using standard Born-Mayer parameters given in Table I. The largest ion displacements are 0.02 Å for NaBr, 0.02 Å for NaCl, and 0.03 Å for NaF. The net change in energy from the perfect lattice sites is no larger than 0.03 eV. When no Born-Mayer potential was used at the surface, the ionic displacements were considerably larger (as large as 0.2 Å). Table II shows the perfect lattice sites and displacements obtained for  $Na_{10}F_2$  as a representative example. The small displacements from the perfect lattice sites indicate that our equilibrium representation is stable

TABLE I. Lattice parameter  $a$  and Born-Mayer potentials used in the CADPAC calculation.

	$a$ (Å)	$A$ (eV)	$\rho$ (Å)
NaF	2.294	670.0	0.290
NaCl	2.820	1102.86	0.321
NaBr	2.953	1384.0	0.328
LiCl	2.571	509.83	0.330

TABLE II. Perfect lattice simulation with the CADPAC. Computed displacements of ions are given (in units of the lattice parameter) for NaF. For simplicity, only one ion of each group of equivalent ions is shown.

Ion	Perfect positions	Displacement
F	(0,0,0)	(0.0041,0.0041,0.0000)
Na	(0,1,0)	(0.0071,0.0071,0.0000)
Na	(-1,0,0)	(0.0125,0.0100,0.0000)
Na	(0,0,1)	(0.0022,0.0022,-0.0059)

and realistic. We have also examined the effect of the size of the array of fixed point ions. When the number of ions was varied from 888 to 1308 for NaF clusters, the absolute energy of the embedded cluster with the triplet STE varied by a few eV. Apart from this constant (to within 0.05 eV) shift of the cluster energy, the calculated APES remained unchanged throughout the range of the configuration coordinate studied. All data reported in this work were obtained with the array of 888 point ions.

Consider the *ab initio* computational procedure. In all of our work, we first compute the eigenvectors for the ground electronic state for a particular geometry arrangement of the ions. The eigenvectors are then used as a starting point for the excited triplet state or singlet state using the unrestricted Hartree-Fock or open-singlet procedures. The eigenvectors resulting from this computation are inspected to ensure that the lowest excited state of interest is treated. The use of ground-state eigenvectors to initiate the excited states as mentioned above is important. In some cases, as will be described in Sec. III C below, bypassing this step led to a different state of the STE with a very different structure characterized by the excited electron abandoning the attractive anion vacancy. Now the gradient-optimization procedure is employed and typically ten cycles are required to find equilibrium positions of the ions in the cluster. It took typically 20 h of CPU time for determining one point on the APES with our SCS-40 computer.

We have employed a variety of basis sets in these computations. The Na basis set is (533/5) taken from Huzinaga<sup>20</sup> and we have split the outer  $s$  functions as (5321/5). We employ 321G and double- $\zeta$  (DZ) (6111/41) basis for F, 631G and double- $\zeta$  (531111/4211) basis for Cl, and (4333/433/4) from Huzinaga<sup>20</sup> with and without split outer  $p$  functions for Br. In this work we report results obtained using DZ for F, 631G for Cl, and (4333/433/4) for Br unless otherwise noted. Although different basis sets produce differences in the total energy of the quantum cluster, the results on the APES were consistent.

The excited electron is, in principle, represented by the cation valence state orbitals. It has been learned, however, through earlier applications of the extended-ion method as well as *ab initio* methods, that additional floating Gaussian orbital basis functions properly placed around the defect add considerable variational freedom. Following this, we have placed a pair of FGO's near the perfect site of the halide ions of the  $V_K$  center. The FGO's are at a distance of 0.3 Å from the regular anion site on the molecular ion axis. As we will see in Sec. III,

this procedure is very efficient in localizing the excited electron around the nascent vacancy and consequently leads to lower total energy. The exponent of these FGO's is 0.08 [in (Bohr radius)<sup>-2</sup>] as has been optimized in earlier calculations.<sup>1</sup> All calculations employ this set of FGO's unless otherwise noted. In recent works Shluger *et al.* have employed 10 or 14 FGO's placed on or near interstitial sites around the  $V_K$  center.<sup>2,18</sup> In order to understand the discrepancies noted between their work and the present work, we have also determined the APES of the triplet STE in NaF using their ten-FGO basis.

The physics of the method described above is fairly straightforward. The array of fixed ions provides a Coulomb potential to the quantum-mechanical cluster ions and the short-range Born-Mayer terms prevent the surface ions of the cluster from undergoing unphysical displacement. This disposition is seen to work satisfactorily as we described above regarding the stability of the perfect lattice simulated by the quantum cluster. The major deficiency in this approach is the absence of any polarization outside the quantum cluster. The fact that the system under study is electrically neutral is a mitigating circumstance. The ICECAP procedure<sup>21</sup> includes this effect while allowing self-consistency to be achieved between the quantum-mechanical cluster and the surrounding ions represented by the shell model of lattice vibration. In practice, this is a complex procedure.

The procedure employed in the ICECAP code is described in earlier references.<sup>21</sup> The calculation is performed for a particular geometry of the quantum-mechanical ions in which an initial charge distribution is assumed. This charge distribution is employed to produce a distribution and polarization of the classical shell model ions which acts on the quantum ions. If the resulting charge distribution computed for the quantum ions differs from the starting distribution, the procedure is repeated until self-consistency is reached. We employ norm-conserving pseudopotentials<sup>22</sup> to represent the Na ion with the valence basis sets taken from Huzinaga. Fluoride ions are represented by a basis set taken from Huzinaga. We employ the terminology ICECAP or CADPAC calculations in this text since these represent a simple shorthand, which describes a type of calculation. Our results of calculations are not a general commentary on the relative merits of either code since this task is well beyond the scope of the present study, which is limited to a specific type of defect.

### III. RESULTS AND DISCUSSION

#### A. Adiabatic-potential-energy surface of the STE in NaF, NaCl, and NaBr

The earlier *ab initio* cluster calculations have established the basic fact that the STE is unstable in the  $D_{2h}$  symmetry and as a consequence undergoes a spontaneous symmetry-breaking relaxation.<sup>1,2</sup> The structure of the STE in the lattice is equivalent to a primitive  $F-H$  pair. We find that the APES's of both spin states show first a drop in energy, then a very small energy variation with axial displacement of the  $V_K$  center for as far as the

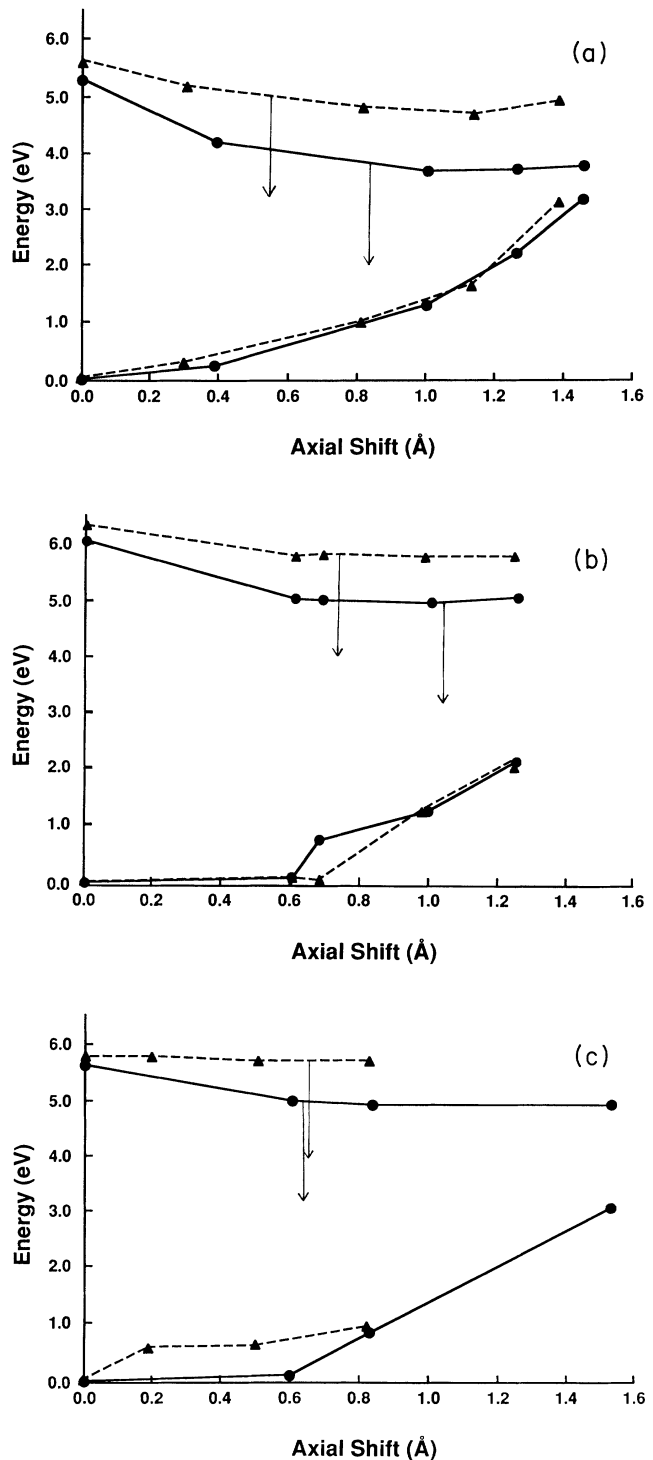


FIG. 2. The adiabatic-potential-energy surfaces of the ground state and of the spin-singlet and -triplet STE's are plotted as a function of the axial shift  $\Delta Q_2$  in (a) NaF, (b) NaCl, and (c) NaBr. The zero of energies is taken at the recombined state in the  $D_{2h}$  symmetry, with the values  $-49\,569.63$ ,  $-69\,136.34$ , and  $-183\,995.81$  eV for NaF, NaCl, and NaBr, respectively. Data points with triangles and circles are, respectively, the spin-singlet and -triplet STE states. The vertical arrows are drawn to indicate the position where the emission energies corresponding to the experimental data of the  $\sigma$  and  $\pi$  bands would match the calculated values. Energy is in eV and  $\Delta Q_2$  in Å.

nearest-neighbor  $F-H$  pair configuration. The results are presented in Fig. 2. The energy is relative to the recombined ground state in the  $D_{2h}$  symmetry. The Franck-Condon ground state reached from the excited state is shown in these figures so that it is possible to infer the luminescence energies of both singlet and triplet STE's. The results shown in Fig. 2 can be summarized as described below.

(1) In all cases studied, both spin-singlet and -triplet STE's are unstable in the  $D_{2h}$  symmetry. The energy gained in moving to the off-center geometry increases, however, in the order of NaBr, NaCl, and NaF.

(2) The APES is remarkably flat after the initial energy drop. It is not easy to pinpoint the location of the absolute minimum. It is likely that there are several local minima. These local minima are believed to correspond approximately to ideal nearest and next-nearest  $F-H$  pairs.

(3) The spin-singlet state behaves somewhat differently from the spin-triplet state. The singlet energy is higher by a fraction of an eV. Also, the location of the APES minimum appears at different values of  $\Delta Q_2$ .

(4) Table III presents the emission energy data ob-

tained in this work. Given the flatness of the computed excited-state potential curves, and the uncertainties inherent in these computations, the actual minima of these curves could in fact lie within a range of  $\Delta Q_2$  of about 0.5 Å and still be consistent with our computed results. The positions of the excited-state minima which would give the emission energies in agreement with experimental data are indicated in Fig. 2 by arrows. It is intended merely to help a comparison between the computed energy curves and the experimental transition energies. Large differences in energy between the  $\pi$  and  $\sigma$  bands observed in many alkali halides, including NaF and NaCl, are attributed to the slight difference in the location of the minima in the configuration-coordinate diagram as well as to the larger energy drop of the triplet STE accompanying the off-center relaxation, as can be seen in Fig. 2. On the basis of this work, we believe that the  $\sigma$  bands originate from the spin-singlet state of the same orbital state as the triplet state, which is responsible for the  $\pi$  bands. This was the recent conjecture presented by both Kan'no *et al.*<sup>23</sup> and Kayanuma<sup>24</sup> based on an overall review of luminescence data for pure and alloyed alkali halide systems.

TABLE III. The calculated recombination energy  $E_{em}$  is given in eV as a function of the off-center shift  $\Delta Q_2$  (in Å), with the experimental data inside the bracket.  $\Delta Q_2^{NN}$  is the value corresponding to the ideal nearest-neighbor separation of the  $F-H$  pairs. This table is to be studied together with Fig. 2.

NaF ( $\Delta Q_2^{NN} = 1.64$ Å)					
S=1					
$\Delta Q_2$ (Å)	0.0	0.39	1.00	1.26	1.45
$E_{em}$ (eV)	5.2	3.98	2.40	1.51	0.60
$\pi$ band (eV)			(2.7)		
S=0					
$\Delta Q_2$ (Å)	0.0	0.30	0.81	1.13	1.37
$E_{em}$ (eV)	5.61	4.91	3.83	3.06	1.64
$\sigma$ band (eV)			(4.27)		
NaCl ( $\Delta Q_2^{NN} = 2.00$ Å)					
S=1					
$\Delta Q_2$ (Å)	0.00	0.60	0.68	0.99	1.24
$E_{em}$ (eV)	6.05	4.97	4.36	3.84	2.87
$\pi$ band			(3.35-3.47)		
S=0					
$\Delta Q_2$ (Å)	0.00	0.60	0.68	0.97	1.23
$E_{em}$ (eV)	6.31	5.70	5.07	4.52	3.64
$\sigma$ band			(5.35-5.6)		
NaBr ( $\Delta Q_2^{NN} = 2.11$ Å)					
S=1					
$\Delta Q_2$ (Å)	0.00	0.60	0.83	1.52	
$E_{em}$ (eV)	5.61	4.91	4.09	1.86	
$\pi$ band			(4.60-4.65)		
S=0					
$\Delta Q_2$ (Å)	0.00	0.20	0.50	0.82	
$E_{em}$ (eV)	5.77	5.16	5.10	4.77	
$\sigma$ band			(4.6)		

The very soft dependence of the excited-state energies on the configuration coordinate  $\Delta Q_2$  deserves a comment regarding the emission bandwidth. A recent model analysis of the shape of the  $\pi$  luminescence band in NaCl by Suzuki *et al.*<sup>8</sup> shows that the evolution of the  $\pi$ -band shape as a function of temperature can be accounted for quantitatively by considering exciton coupling to a soft phonon mode ( $Q_2$  mode) as well as to the stiff stretching mode of the molecular ion ( $Q_1$  mode). They find phonon energies of 2.2 and 7.9 meV for the soft mode, respectively, in the excited triplet and ground states by fitting to the experimental data. This soft mode is attributed to the axial translational mode of the STE. The corresponding force constants of the soft mode are 0.08 and 1.08 eV/Å<sup>2</sup>, respectively, for the excited and ground states. Although we have not attempted an evaluation of the force constants in the present calculation, a crude estimate of the force constants can be made for the ground state. This gives 2.8 eV/Å<sup>2</sup> for NaF and comparable values are obtained for the other two after curve smoothing. This value is in order-of-magnitude agreement with the above fitted value of Ref. 8. As for the excited state, our data are inadequate for a similar estimate. Regarding the emission bandwidth, the present work is not incompatible with the result of analysis given in Ref. 8.

(5) It is noted that the ground and excited triplet states' APES's cross in NaF, Fig. 2(a), at around the first-nearest-neighbor  $F$ - $H$  separation. In NaCl and NaBr we do not observe similar trends. A comparison of Figs. 2(a)–2(c) shows that this is the result of the larger energy drop of the triplet APES observed in NaF. This difference is significant in understanding the  $\pi$ -emission-band quenching, which will be analyzed in Sec. III C.

In order to investigate the energy surface connecting the STE and  $F$ - $H$  pairs of varying separation, we have extended the range of axial shift for NaF employing the larger quantum cluster Na<sub>14</sub>F<sub>3</sub>. For this study, we started from a finite off-center geometry. The total energy of

the triplet STE and the Mulliken population (on the three halide ions and of the pair of floating Gaussians inside the quantum cluster) as a function of the position of the center of gravity of the hole charge distribution  $\Delta Q_2^{cm}$  are presented in Table IV. The Franck-Condon ground-state energy is also given. From this set of computations, we have confirmed that the triplet STE APES remains very flat after the initial energy drop to within about 0.2 eV all the way to the second-nearest-neighbor  $F$ - $H$  pair configuration. It seems likely that there are several local minima on the multidimensional energy surface, which are separated by small energy barriers of the order of 0.1 eV, in agreement with inferences made from luminescence data.<sup>25,26</sup> The Mulliken population  $\{q_i\}$  obtained with the cluster Na<sub>14</sub>F<sub>3</sub> over the same range of  $\Delta Q_2$  shows that the self-trapped hole diffuses along the halide ion row with a small activation energy. It is expected that the hole population is about equally distributed on a pair of fluoride ions when the  $H$  center is near the ideal nearest-neighbor location ( $\Delta Q_2 = 1.6$  Å). Away from this site, the hole is strongly polarized, mainly because of the inequivalent Madelung potential on the two sites. It is remarkable, by contrast, that the excited electron remains localized on the anion vacancy as soon as the molecular ion F<sub>2</sub><sup>-</sup> has slipped off center.

We have also studied the triplet STE using the ICECAP code. This code addresses the problem of the embedding lattice in terms of the HADES code which is interfaced with a UHF code. The charge distribution inside the quantum cluster and the response of the embedding lattice have to be handled in a self-consistent way by iterating a number of times until convergence. We have already given some details regarding the basis used in Sec. II. A pair of FGO's positioned near the anion vacancy was used to augment the excited electron basis as in the above work with the CADPAC code. In regard to the charge consistency, we have considered up to the quadrupole moments. Our attempts to achieve a self-consistent

TABLE IV. Energy  $E_t$  of the triplet state STE obtained with the cluster Na<sub>14</sub>F<sub>3</sub> is given as a function of the axial shift  $\Delta Q_2$  (the midpoint of the molecule bond). The ground-state energy  $E_0$  is also given as a function of  $\Delta Q_2$ . Energy values are reported relative to the ground-state energy of the first entry which is  $-69\,972.59$  eV. The axial shift of the center of gravity of the hole charge distributed on the three F ions  $\Delta Q_2^{cm}$  is also given to indicate the diffusion of the hole. It is seen that the ground state crosses the excited-state energy surface at around  $\Delta Q_2^{cm} = 2$  Å. The Mulliken population is given for the three F ions which share the hole and the two FGO's on which the excited electron is principally located. The surrounding Na ions also share a small part of the electron. FG<sub>1</sub>, FG<sub>2</sub>, F1, F2, and F3 are as defined in Fig. 1.

$\Delta Q_2$ (Å)	0.53	1.05	1.51	1.84	2.03	4.23
$\Delta Q_2^{cm}$ (Å)	-0.44	0.25	1.15	2.56	2.86	3.15
$E_t$ (eV)	5.30	5.28	5.46	5.37	5.37	5.39
$E_0$ (eV)	0.00	1.99	4.41		(crosses the excited state)	
	Mulliken population					
FG <sub>1</sub>	0.064	0.055	0.045	0.050	0.054	0.059
FG <sub>2</sub>	0.676	0.870	0.923	0.929	0.941	0.953
F1	9.879	9.848	9.677	9.125	9.093	9.092
F2	8.995	9.049	9.247	9.812	9.854	9.878
F3	9.945	9.946	9.945	9.929	9.915	9.892

TABLE V. Total energy of the spin-triplet STE in NaF calculated with the ICECAP code using the positions of atoms optimized with the CADPAC code. Use of a pseudopotential for Na ion removes the core electrons, and therefore it is meaningless to compare the total energy given here with the total energy obtained with the CADPAC calculation.

$\Delta Q_2$ (Å)	0.0	0.09	0.40	0.80	1.00	1.30
$E_i$ (eV)	-5398.50	-5401.42	-5401.35	-5402.41	-5403.07	-5402.56

geometry optimization for the off-center configurations have not been successful. At an approximate level we kept the cations fixed on their normal lattice sites while we varied the positions of the halide ions so as to attain an energy minimum. This procedure gave comparable energy changes in the APES and the same electron-hole polarization pattern as we described above in connection with the calculations using the fixed point-ion embedding cluster. As a further test, we have used the positions of ions optimized in the CADPAC work for NaF and ran the ICECAP code to obtain the total energy including the lattice polarization. This result is shown in Table V. It confirms well the energy drop which we obtained already in Ref. 1. For an axial shift of  $F_2^-$  between 1.0 and 1.3 Å the energy rises by about 0.5 eV. It is not clear whether or not this is an effect of the small cluster size in comparison with the large axial shift (which is close to the ideal nearest-neighbor separation of 1.6 Å).

The present *ab initio* calculations of the STE in three sodium halides confirm the earlier results of Song and co-workers based on the extended-ion approach.<sup>3,4</sup> This includes the basic adiabatic instability of the on-center STE, the large energy gain in the off-center geometry, and the very flat potential-energy surface for further separation of the electron and hole. These results explain a host of apparently confusing experimental data regarding the strong material dependence of the Stokes shift of  $\pi$  bands, triplet STE lifetime, and low-temperature  $F$ -center-formation yield as characterized by the Rabin and Klick diagram. A larger off-center shift  $\Delta Q_2$ , as in NaF (a type III according to Kan'no, Tanaka, and Hayashi<sup>9</sup>) leads to a larger Stokes shift and a longer triplet lifetime of the  $\pi$  band. In NaBr, a typical material of type I,  $\Delta Q_2$  is definitely smaller than in NaF and responsible for the smaller Stokes shift and shorter lifetime. NaCl (an example of type II) is an intermediate case. The strong material dependence of the low-temperature  $F$ -center-production yield under ionizing radiation as observed in the Rabin and Klick diagram<sup>15</sup> was attributed to the difference in the relaxation energy available along the [110] axis.<sup>3</sup> The present work confirms the earlier results and supports the analysis of Ref. 3. Several recent review papers have presented unified analyses of experimental data regarding the STE and  $F$ -center formation.<sup>17,19,27</sup> More recent experimental data provide additional information. Resonant Raman scattering experiments show that the hole component of the STE in NaCl has its stretching mode frequency very close to that of the  $H$  center ( $360 \text{ cm}^{-1}$  which is much larger than that of the  $V_K$  center at  $240 \text{ cm}^{-1}$ ), while the electron excited Raman scattering presents spectra strikingly similar to that of the  $F$  center.<sup>7</sup>

### B. Influence of the FGO basis sets on APES

Shluger *et al.* have presented a detailed account of their study of the triplet STE in KCl using the ICECAP code.<sup>2</sup> The results of their work based on the ICECAP code are in general agreement with those of our earlier work as well as the present work using the CADPAC code. Both studies predict instability of the STE in the on-center geometry and a clear localization of the excited electron charge density in the off-center geometry. There is also agreement regarding the strong correlation between the hole and excited electron. One major point of disagreement between our work and that of Ref. 2 is found regarding the adiabatic potential energy of the STE for further separation of the electron and hole. Indeed, a potential barrier of 0.7 eV or more is predicted in Ref. 2, while a very flat potential is obtained by us as shown in Table IV and Fig. 2. This difference is of substantial importance, as it should influence the subsequent evolution of the off-center STE.

We have therefore undertaken further studies in order to understand this disagreement. We have run the CADPAC code for the cluster  $\text{Na}_{10}\text{F}_2$  using the FGO basis which has been used in Ref. 2. In the following, we give some detail of the comparative studies. We note that NaF and KCl belong to the same group of STE's (Refs. 9 and 17) in terms of the large Stokes shift, efficient low-temperature  $F$ -center formation, and the Rabin-Klick parameter  $S/D$  among other parameters. Several sets of FGO basis have been used by Shluger *et al.* Most of the work reported is with ten FGO's positioned at interstitial sites, some of which are optimized.<sup>2</sup> We construct two basis sets from the ten-FGO basis set described in Table III of Ref. 18. Here the halide ion sites are (0.5,0.5,0.0) and (-0.5,-0.5,0.0) in units of the anion-cation distance. The first set of FGO's is positioned at (0.95,0.95,0.0), (-0.95,-0.95,0.0), and ( $\pm 0.95, \pm 0.04, \pm 0.50$ ) taken from Ref. 18. A second set was constructed with the coordinates in the  $D_{2h}$  symmetry and positioned symmetrically along the (110) axis. The second set of functions is positioned at (0.95,0.95,0.0), (-0.95,-0.95,0.0), (0.95,0.04, $\pm 0.50$ ), (0.04,0.95, $\pm 0.50$ ), (-0.04,-0.95, $\pm 0.50$ ), and (-0.95,-0.04, $\pm 0.50$ ). We have examined both sets of ten FGO's which we label as no. 1 and no. 2 basis. For comparisons, we have created a third set of ten FGO's. In this basis set, the first group of two FGO's along the molecule axis is replaced by the pair of FGO's which are located near the anion sites and which we have been using. This basis set is labeled no. 3, and is close to that used in Ref. 2 for large off-center geometry. Three points on the APES are evaluated with separate geometry optimizations with

TABLE VI. Comparative study of the ten FGO basis set used in Ref. 2 applied to the triplet STE in NaF. No. 1, no. 2, and no. 3 basis sets are various combinations of two axial FGO's and eight interstitial FGO's as explained in the text. Total energy  $E_t$  is given in eV and  $\Delta Q_2$  is given in angstroms.

		$\Delta Q_2$ $E_t$	$\Delta Q_2$ $E_t$	$\Delta Q_2$ $E_t$
2 FGO		0.0 -49 563.65	0.90 -49 565.20	1.32 -49 565.04
10 FGO	no. 1	0.0 -49 563.72		1.32 -49 564.55
10 FGO	no. 2	0.0 -49 563.84	0.72 -49 565.07	1.32 -49 564.67
10 FGO	no. 3	0.0 -49 563.85	0.72 -49 565.13	1.32 -49 565.33

each of no. 2 and no. 3 basis sets. For the no. 1 set, we have merely evaluated the cluster energy using the atom positions obtained with our original two FGO basis set. All the results are collected in Table VI. For comparison, we have included also the energies obtained above with our original two FGO's.

The main points of this comparative study are the following.

(1) Our original pair of FGO's placed near the anion vacancy gives lower energy compared to basis sets no. 1 and no. 2 with ten FGO's, except in the on-center geometry. The use of the interstitial FGO's spread around the molecular ion gives a lower energy of about 0.2 eV when in the on-center geometry. This is not unexpected, because it has been shown by various calculations that the excited electron of the STE of the lowest triplet state occupies a diffuse orbital in the  $D_{2h}$  symmetry.<sup>1,2,4</sup>

(2) Most important is that a potential barrier of 0.4 eV appears between  $\Delta Q_2=0.7$  and 1.3 Å with no. 2 FGO basis. When our original two FGO's are included in the basis set, the barrier is either eliminated completely (as with no. 3), or reduced to about 0.2 eV when used alone.

(3) On examining the Mulliken population, we observed that the inclusion of the pair of FGO's close to the anion vacancy assists in the localization of the excited electron and contributes to lowering the energy in the off-center geometry.

From this study it is clear that the choice of the floating Gaussian basis representing the excited electron is important for obtaining the correct adiabatic potential energy. We believe that the choice of FGO basis positions near normal anion lattice sites is a crucial factor in allowing the excited electron to become localized on the nascent anion vacancy and thus provides the driving force for off-center displacement resulting in the flat APES surfaces. There are other factors, however, which are different in the two calculations and which we cannot exclude from having possible influence. These include the basis-set choice which involves pseudopotentials in Ref. 2 as compared to full basis sets here, lattice-ion polarization effects which are treated at different levels of approximation, and the actual geometry optimization procedure

for the quantum cluster which is achieved differently in the two studies. We have also reservations on the procedure used in Ref. 2 in representing the localized excited electron (as equally divided fractional charges distributed on the ten FGO's) and representing the strongly polarized molecular ion (as a pair of  $-e/2$  charges) in the HADES part of the computation. Further work would be needed to assess these possible factors.

### C. Study of the STE in LiCl

Lithium halides generally exhibit trends of type-II materials which include NaCl.<sup>28</sup> Earlier, Shluger, Grimes, and Catlow have presented work on LiCl (Ref. 18) based on the ICECAP code. Their results can be summarized as follows.

(1) The stable structure of the triplet STE is off center, with a very small value of  $\Delta Q_2$ , about 0.07 Å. The energy gain from the on-center geometry is about 0.15 eV.

(2) The excited electron and hole correlate strongly as in other alkali halides. However, the excited electron is not localized on the nascent anion vacancy as expected, but instead is in an extended orbital centered at the opposite end from the nascent anion vacancy across the molecular ion. The hole is extremely polarized such that the Cl ion proximal to the excited electron is found to be Cl.<sup>0.045-</sup>

(3) A structure more like the off-center STE found in other systems with the excited electron localized on the nascent anion vacancy is found to be less than about 0.8 eV higher in energy than the above structure. They reported that whichever structure is obtained depends on the initial eigenvectors used in initiating the self-consistent-field procedure.

In view of the STE structure with the excited electron in a diffuse orbital reported in Ref. 18, we have investigated the triplet state STE in LiCl using the cluster  $\text{Li}_{10}\text{Cl}_2$  with the CADPAC code. The basis used for Li is (1111),<sup>20</sup> while for Cl the same basis set is used as in NaCl work. A pair of FGO's is placed near the anion vacancies as in other work. This calculation shows that the triplet STE energy surface is very flat after an initial ener-



TABLE VII. Total energy of the triplet STE in LiCl obtained with the CADPAC code for the cluster  $\text{Li}_{10}\text{Cl}_2$ . The axial shift  $\Delta Q_2$  is in Å and the total energy  $E_t$  is in eV.

$\Delta Q_2$	0.00	0.29	0.47	0.70
$E_t$	-27 134.50	-27 134.97	-27 134.99	-27 135.03

gy drop of about 0.5 eV. Within about 0.05 eV we do not note any energy variation up to an axial shift of about 0.7 Å. The hole is strongly polarized and the excited electron is localized on the nascent anion vacancy as in all other systems. The results are shown in Table VII where the total energy of the cluster is given as a function of the axial shift  $\Delta Q_2$ . We have investigated the occurrence of the unexpected solution in the SCF procedure as reported in Ref. 18, namely, the one with the excited electron leaving the attractive anion vacancy and occupying a diffuse state. In all of the present calculations with the CADPAC code, we first determined the eigenvectors for the recombined singlet state (the ground state of the cluster). These eigenvectors were then used to compute the excited states of the cluster. This procedure always gave the normal structure in LiCl. When this procedure was not followed and the triplet STE state was calculated without ground-state eigenvectors as the initial vectors, the peculiar solution mentioned above was obtained in NaF with small  $\Delta Q_2$  (about 0.1 Å). This solution has, however, an energy higher than the "normal" one by about 0.9 eV in our work. At larger values of  $\Delta Q_2$  ( $> 0.8$  Å), independent of the initial eigenvectors used, the normal solution was always obtained. It seems that the dependence on the initial eigenvectors of the solution obtained in the SCF calculation is of a technical nature, as long as the lowest-energy solution is retained at the end. It seems that the choice of the FGO basis has an influence on whether one type of solution or the other has a lower energy even in this context.

#### D. Mechanisms of $\pi$ emission quenching

We now present a model to explain the quenching of the  $\pi$  band in alkali halides. There are two distinct groups regarding the quenching as a function of temperature as has been analyzed in a recent paper by Itoh, Eshita, and Williams.<sup>29</sup> In NaCl, NaBr, KI, and RbI, the  $\pi$ -band intensity and  $F$ -center-formation yield are anticorrelated as a function of the temperature.<sup>10</sup> In the second group, which includes KCl and KBr, there is no anticorrelation. Instead, there is nonzero  $F$ -center-production yield even at liquid-He temperature which increases further with increasing temperature. The  $\pi$  band is quenched at a low temperature (typically 10–20 K), which is lower than that where the  $F$ -center yield starts to increase. The first group includes types I and II of the classification of Kan'no, Tanaka, and Hayashi,<sup>9</sup> while the second group corresponds to type III. Itoh *et al.* have argued that nonradiative decay of the STE to the ground state may be different in these two groups.

From Fig. 2 and Table IV, it clearly appears that in NaF, a typical type-III material, the ground-state APES crosses the excited APES close to the nearest-neighbor

$F$ - $H$  configuration, while for NaCl and NaBr, respectively, types II and I, no crossing of ground and excited states is observed within the range of  $\Delta Q_2$  investigated. This difference is explained as follows. As can be seen in Fig. 2, the ground-state APES rises with a comparable rate in all three materials studied. On the other hand, the triplet state APES shows a different amount of energy drop for the three materials studied (about 1.5 eV in NaF, 1 eV in NaCl, and 0.5 eV in NaBr) when the triplet STE undergoes off-center relaxation. We propose that this is at the origin of different luminescence quenching as a function of temperature. It seems reasonable to argue that in NaF and other type-III materials,  $\pi$  emission is quenched primarily by a nonradiative transition to the ground state occurring before the system evolves to a well separated  $F$ - $H$  pair. There is, however, a finite probability of achieving a well separated  $F$ - $H$  pair even at low temperatures due to the substantial kinetic energy available along the (110) axis, as was argued in Ref. 3. When the temperature is raised, even after the  $\pi$  emission is practically quenched, a thermally activated  $F$ -center production can be observed as the system overcomes the small potential barrier which exists on the path of large  $F$ - $H$  separation. On the other hand, in type-I and -II materials, the ground state does not cross (or does not cross until larger values of  $\Delta Q_2$ ), and as a result the  $\pi$  emission is in direct competition with thermal  $F$ -center formation. The kinetic energy available along the defect process coordinate (110) is smaller for these materials, as can be seen in Fig. 2. In these materials, low-temperature  $F$ -center formation is very inefficient. The analysis presented earlier by Itoh, Eshita, and Williams<sup>29</sup> on empirical grounds is now explained by the present *ab initio* calculation. The APES calculated in the present work supports the two types of APES proposed earlier by Song and Kayanuma to explain the quenching.<sup>17,24</sup>

#### IV. CONCLUSION

In this work we presented a detailed account of the adiabatic-potential-energy surface connecting the STE and  $F$ - $H$  pair based on *ab initio* Hartree-Fock cluster calculations in several typical alkali halides. We found that the energy gain achieved when the STE relaxes in the off-center geometry, as well as the off-center shift  $\Delta Q_2$ , depend on the alkali halides. Both the energy drop and the axial shift  $\Delta Q_2$  are large in NaF [an example of type-III STE (Ref. 9)] and small in NaBr (an example of type-I STE). NaCl, a type-II material, is an intermediate case. After the initial energy drop, the APES remains remarkably flat and we found no energy barrier larger than about 0.2 eV between the STE, which is already a primitive nearest-neighbor  $F$ - $H$  pair, and further separated  $F$ - $H$  center pair.

From the present calculation we proposed that the  $\sigma$  polarized emission band is the recombination luminescence of the spin-singlet state belonging to the same STE orbital state as the triplet state responsible for the  $\pi$  bands. Given the difficulties inherent in an *ab initio* calculation of the STE, the degree of agreement between the theoretical transition energies and experimental data is reasonable for both bands. The energy difference between the  $\sigma$  and  $\pi$  bands is attributed to the different off-center shifts at equilibrium of the spin-singlet and -triplet states as well as to the larger energy drop of the triplet STE associated with the off-center relaxation. We have also proposed a model for the  $\pi$ -band quenching based on the calculated APES. Our model is in agreement with a recent analysis based on experimental data. It also establishes, in a simple and consistent manner, a correspondence between the various classifications proposed for the  $\pi$ -band quenching<sup>29</sup> on the one hand and the  $\pi$ -band Stokes shift<sup>9</sup> and low-temperature *F*-center-production

yield<sup>15</sup> on the other. An important element which divides the STE in alkali halides into two or three groups is the off-center axial shift  $\Delta Q_2$  and the associated relaxation energy. On the basis of the off-center STE model, it is possible to present a unifying picture of the STE regarding all of the above-mentioned properties.<sup>17,19,27</sup>

The convergence noted between the *ab initio* and the extended-ion approaches employed in earlier works<sup>3,4</sup> regarding the off-center configuration of the STE and its evolution towards a Frenkel defect pair is remarkable indeed when the difference in the methods is taken into account. The key in the study of the STE is in a correct treatment of the interaction of the excited electron with the lattice ions. The excited electron is the principal element which induces the large atomic rearrangement in the lattice by localizing on the vacant anion site. This mechanism seems more universal than is generally recognized, as can be seen in recent calculations of the STE in SiO<sub>2</sub>.<sup>30,31</sup>

- 
- <sup>1</sup>R. Baetzold and K. S. Song, *J. Phys. Condens. Matter* **3**, 2499 (1991).
- <sup>2</sup>A. L. Shluger, N. Itoh, V. E. Puchin, and E. N. Heifets, *Phys. Rev. B* **44**, 1499 (1991).
- <sup>3</sup>K. S. Song, C. H. Leung, and R. T. Williams, *J. Phys. Condens. Matter* **1**, 683 (1989).
- <sup>4</sup>K. S. Song and C. H. Leung, *J. Phys. Condens. Matter* **1**, 8425 (1989).
- <sup>5</sup>R. T. Williams, B. B. Craig, and W. L. Faust, *Phys. Rev. Lett.* **52**, 1709 (1984).
- <sup>6</sup>T. Tokizaki, T. Makimura, H. Akiyama, S. Iwai, A. Nakamura, K. Tanimura, and N. Itoh, *Phys. Rev. Lett.* **67**, 2701 (1991).
- <sup>7</sup>K. Tanimura, T. Suzuki, and N. Itoh, *Phys. Rev. Lett.* **68**, 635 (1992).
- <sup>8</sup>S. Suzuki, K. Tanimura, N. Itoh, and K. S. Song, *J. Phys. Condens. Matter* **1**, 6993 (1989).
- <sup>9</sup>K. Kan'no, K. Tanaka, and T. Hayashi, *Rev. Solid State Sci.* **4**, 383 (1990).
- <sup>10</sup>D. Pooley and W. A. Runciman, *J. Phys. C* **3**, 1815 (1970).
- <sup>11</sup>N. Itoh and M. Saidoh, *J. Phys. (Paris) Colloq.* **34**, C9-101 (1973).
- <sup>12</sup>N. Itoh, A. M. Stoneham, and A. H. Harker, *J. Phys. C* **10**, 4197 (1977).
- <sup>13</sup>M. N. Kabler, *Phys. Rev.* **136**, A1296 (1964).
- <sup>14</sup>R. D. Amos and J. E. Rice, CADPAC: The Cambridge Analytical Derivatives Package issue 4.0 (unpublished).
- <sup>15</sup>H. Rabin and C. C. Klick, *Phys. Rev.* **117**, 1005 (1960); P. D. Townsend, *J. Phys. C* **6**, 961 (1973).
- <sup>16</sup>A. L. Shluger (private communication).
- <sup>17</sup>K. S. Song and Y. Kayanuma, *Butsuri* **45**, 469 (1990) (in Japanese).
- <sup>18</sup>A. L. Shluger, R. W. Grimes, and C. R. A. Catlow, *J. Phys. Condens. Matter* **3**, 3125 (1991).
- <sup>19</sup>K. S. Song and C. H. Leung, *Rev. Solid State Sci.* **4**, 357 (1990).
- <sup>20</sup>S. Huzinaga, *Gaussian Basis Sets for Molecular Calculations* (Elsevier, New York, 1984).
- <sup>21</sup>A recent review which references the many contributions to this method is J. M. Vail, *J. Phys. Chem. Solids* **51**, 589 (1990).
- <sup>22</sup>G. R. Bachelet, D. R. Haman, and M. Schluter, *Phys. Rev. B* **26**, 4199 (1982).
- <sup>23</sup>K. Kan'no, K. Tanaka, H. Kosaka, Y. Nakai, M. Itoh, T. Miyayaga, K. Fukui, and M. Watanabe, *Phys. Scr.* **41**, 120 (1990).
- <sup>24</sup>Y. Kayanuma, *Rev. Solid State Sci.* **4**, 403 (1990).
- <sup>25</sup>T. Eshita, K. Tanimura, N. Itoh, and H. Nishimura, *J. Phys. Soc. Jpn.* **54**, 4418 (1985).
- <sup>26</sup>R. T. Williams, H. Liu, G. P. Williams, Jr., and K. J. Platt, *Phys. Rev. Lett.* **66**, 2140 (1991).
- <sup>27</sup>R. T. Williams and K. S. Song, *J. Phys. Chem. Solids* **51**, 679 (1990).
- <sup>28</sup>K. Tanimura and N. Itoh, *Phys. Rev. B* **45**, 1432 (1992).
- <sup>29</sup>N. Itoh, T. Eshita, and R. T. Williams, *Phys. Rev. B* **34**, 4230 (1986).
- <sup>30</sup>A. L. Shluger and E. Stefanovich, *Phys. Rev. B* **42**, 9664 (1990).
- <sup>31</sup>A. Fisher, W. Hays, and A. M. Stoneham, *Phys. Rev. Lett.* **64**, 2667 (1990).